

May 2013

Monte Carlo Simulation for silicon on silane HWCVD for thin film solar cells

AnnaLeigh Smith
Macalester College, smithannaleigh@gmail.com

Follow this and additional works at: <https://digitalcommons.macalester.edu/mjpa>



Part of the [Astrophysics and Astronomy Commons](#), and the [Physics Commons](#)

Recommended Citation

Smith, AnnaLeigh (2013) "Monte Carlo Simulation for silicon on silane HWCVD for thin film solar cells," *Macalester Journal of Physics and Astronomy*. Vol. 1: Iss. 1, Article 13.
Available at: <https://digitalcommons.macalester.edu/mjpa/vol1/iss1/13>

This Capstone is brought to you for free and open access by the Physics and Astronomy Department at DigitalCommons@Macalester College. It has been accepted for inclusion in Macalester Journal of Physics and Astronomy by an authorized editor of DigitalCommons@Macalester College. For more information, please contact scholarpub@macalester.edu.

Monte Carlo Simulation for silicon on silane HWCVD for thin film solar cells

Abstract

Thin film solar cells offer a viable alternative to crystal silicon solar cells. They are expected to be cheaper to fabricate because they use material more efficiently, and are deposited in a process which can create larger area solar cells [1]. However, a high deposition rate is necessary for economic viability. A Monte Carlo simulation can model the molecular interactions in hot wire chemical vapor deposition and track the position and velocity distribution of molecular species in the gas [2]. Determining the flux on the substrate can help us to increase deposition rate by adjusting control parameters accordingly [3]. As a preliminary step, we compare thermalization properties of different intermolecular models to assess suitability for a gas phase scattering model.

Cover Page Footnote

Advisor: James Doyle Macalester College

Monte Carlo Simulation for silicon on silane HWCVD for thin film solar cells

AnnaLeigh Smith
Advisor: James Doyle
Macalester College

Abstract

Thin film solar cells offer a viable alternative to crystal silicon solar cells. They are expected to be cheaper to fabricate because they use material more efficiently, and are deposited in a process which can create larger area solar cells [1]. However, a high deposition rate is necessary for economic viability. A Monte Carlo simulation can model the molecular interactions in hot wire chemical vapor deposition and track the position and velocity distribution of molecular species in the gas [2]. Determining the flux on the substrate can help us to increase deposition rate by adjusting control parameters accordingly [3]. As a preliminary step, we compare thermalization properties of different intermolecular models to assess suitability for a gas phase scattering model.

I Goals

The objective of this project is to compare three kinetic potential models for particle interactions in a Monte Carlo simulation of chemical vapor deposition: the hard sphere model, the Lennard-Jones potential, and the variable soft sphere mode [4]. These models are distinguished by the thermalization behavior of a test particle gas. This behavior is characterized by the evolution of the collision-dependent velocity distribution of the test particles compared to a thermalized background gas. Our preliminary goal is to use this comparison of models to assess suitability for a gas phase scattering model that accurately reflects particle interactions but is computationally inexpensive.

Ultimately, we wish to develop a robust model of film deposition that maximizes deposition rate for high quality silicon films by examining the spatial distribution of molecular species in the deposition chamber.

II Introduction

II.1 Hot Wire Chemical Vapor Deposition

Hot wire chemical vapor deposition (HWCVD) is a process used for growing thin film solar cells [1][3]. A tantalum or tungsten wire runs through a vacuum chamber and is heated to about 2200K [5]. Silane is pumped into the chamber and reacts off the hot wire, immediately resulting in Si and H , with additional reaction yielding H_2 , SiH_3 , Si_2H_2 , and possibly other Si_nH_m species. These molecules experience several thermal collisions before depositing on a glass substrate. See Figure 1 for a full diagram.

Process control parameters in hot wire chemical vapor deposition include gas flow rate, gas pressure, filament temperature, substrate temperature, distance between filament and substrate, dilution in H_2 . These control parameters

affect the production time and quality of the result. Some species produced in this process have lower sticking coefficients than others, where the sticking coefficient is inherent to the molecule and defined as the ratio of adsorbate atoms that "stick" to a surface to the total number of atoms touching the surface [6]. It is preferable for molecules with lower sticking coefficients to land on the substrate because this allows for a more uniform surface distribution, and thereby a more efficient cell. If the distribution of silane species in the chamber is known, then the parameters can be adjusted to optimize the deposition of desired species, increasing the efficiency of cells.

As silane reaches the hot wire, silicon and hydrogen atoms interact with other molecules, the majority of which are at a lower temperature and in a thermalized state [5]. Thus, the system is not in equilibrium. Over time and after a certain number of collisions, the molecules that react off the wire do thermalize to the lower temperature if they don't undergo a chemical reaction. Thus, the molecules undergo both thermal interactions, which change their energy, and chemical interactions that alter their chemical structure. The competition between reaction and thermalization affects the distribution of molecular species in the chamber.

II.2 Molecular Flow Regimes

Two kinetic regimes can be considered in this system of HWCVD for thin film solar cell deposition: diffusive flow where the mean free path l is much less than the distance between the wire and the substrate, and molecular flow, a lower pressure regime where $l \sim L$ [2]. Diffusive flow is well-modeled by the Navier Stokes equations. However, molecular flow must be described with Boltzmann transport equation which cannot be easily solved analytically or numerically [2]:

$$\frac{\partial f}{\partial t} + \frac{\mathbf{p}}{m} \cdot \nabla f + \mathbf{F} \cdot \frac{\partial f}{\partial \mathbf{p}} = \left(\frac{\partial f}{\partial t} \right)_{coll}$$

$$\left(\frac{\partial f}{\partial t} \right)_{coll} = \int \int g I(g, \Omega) [f(\mathbf{p}'_A, t) f(\mathbf{p}'_B, t) - f(\mathbf{p}_A, t) f(\mathbf{p}_B, t)] d\Omega d^3 \mathbf{p}_A$$

An accepted alternative to the Boltzmann transport equation for modeling molecular flow is a Monte Carlo simulation, where individual trajectories of particles are computationally modeled, by thermal interaction with a thermalized background gas, using direct sampling [7].

III Methodology

III.1 Test Particle Monte Carlo

The basic form of a Monte Carlo simulation for gas transport is a test particle interacting with a background gas. This type of simulation tracks individual particle interactions, with the assumption that each particle represents on the order of 10^7 particles [4]. The outcome is a velocity and position distribution of the test particles which is based on their initial energy, the temperature of the background gas, the interaction potential with the background gas, and the pressure in the system.

All test particles are initialized with a single high energy value, 1eV, corresponding to a *Si* molecule that has just interacted with the hot wire. The mean free path is $l = \frac{1}{n\sigma}$, where the maximum impact parameter of the particle, b_{max} , is chosen to be 3.0Å and is on the order of the size of the molecules and n is a function of the pressure and the temperature of the background gas [8]. At every length l the particle interacts with the background gas and experiences a change in its energy and velocity. The test particle Monte Carlo program takes parameters of pressure, temperature, test particle mass, background gas particle mass, and hot wire temperature. This process is iterated for a chosen number of timesteps or collisions. The final position and velocity data for that particle is stored, and then this process is repeated until N particles have been simulated. A flowchart of this process is shown in Figure 2.

The velocity of the background particle is sampled from the Maxwell Boltzmann (MB) velocity distribution at the temperature of the background gas. The MB distribution is determined by

$$P(v) = \frac{4v^2}{\sqrt{\pi}v_0^3} e^{-Mv^2/2kT}$$

where k is the Boltzmann constant, T is the temperature of the background gas, M is the mass of the particle, and $v_0 = \sqrt{\frac{2kT}{M}}$. The mean velocity is v_0 .

Figure 3 shows the algorithm for determining the velocity of a background particle. Two random numbers are generated. RN1 is between 0 and 1, and RN2 is between 0 and the maximum velocity (5 times the average velocity, by convention). This point is plotted on the graph of the normalized MB curve, as in Figure 4. If the point is above the distribution, another random sampling is taken. Otherwise, RN2 is taken for the velocity of the background gas particle. This type of sampling results in an effective MB distribution of the background gas.

The program is tested by running 100000 particles for an increasing number of collisions and plotting a histogram of the final velocity magnitudes against the background gas Maxwell-Boltzmann distribution. As the number of collisions increases, the test particles thermalize with the background gas and the velocity distribution approaches a Maxwell-Boltzmann distribution at the temperature of the background gas.

III.2 Kinematics of Two-Particle Collisions

A primary component of the simulation is the representation of a collision between two particles. Three types of collision models are proposed: hard sphere collision, variable hard sphere collision, and the incorporation of a Lennard-Jones (LJ) potential [4][9]. The hard sphere collision model is used as a precursor to the more complex particle dynamics of the LJ potential and the variable soft sphere potential. It models the particles as engaging in a purely repulsive, elastic collision. The program for modeling a collision takes the two initial velocity vectors as inputs and outputs final, post-collision velocity vectors.

In order to calculate the post-collision velocity, the program changes the frame of reference such that the second particle is stationary and the first particle's total velocity is in the x-direction. The calculations for this coordinate transformation are included in the appendix. The final velocity is calculated for both particles after the collision. The deflection angle is determined by

$$\psi = \tan^{-1} \left(\frac{\sin \theta}{\cos \theta + m_1/m_2} \right)$$

where θ is the deflection angle in the center of mass frame, m_1 is the mass of the test particle and m_2 is the mass of the background gas particle, as shown in Figure 5 [8].

θ is found with the relation $\theta = \pi - 2\Theta$ where

$$\Theta = b \int_{r_0}^{\infty} \frac{dr}{r^2 \left[1 - \frac{V(r)}{E_{COM}} - \left(\frac{b}{r} \right)^2 \right]^{\frac{1}{2}}} \quad (1)$$

where r_0 is the distance of closest approach, E_{COM} is the energy of the test particle in the center of mass frame, and $V(r)$ is the potential energy between the particles [8]. Although the upper limit of the radius of interaction is infinity, we define a parameter b_{max} as the maximum radius at which the particles will interact. This parameter is determined by an arbitrary cutoff of the scattering angle θ at one degree of scattering.

Ultimately θ is a function of the impact parameter b and the energy E . Including molecular potentials in this interaction, b is a function of the energy. For a hard sphere $b_{max} = r_1 + r_2$, where r_1 and r_2 are the radii of the interacting particles.

The final energy of the test particle is

$$T_1 = \left(1 - \frac{2m_1m_2}{(m_1 + m_2)} (1 - \cos \theta) \right) T_0 \quad (2)$$

where T_0 is the initial energy of the test particle. This is the primary equation governing the thermalization process [8].

III.3 Interaction Models

III.3.1 Hard Sphere Model

For a hard sphere it is assumed that each particle has a fixed radius r_1 and r_2 and that they only interact upon physical contact. Then in equation 1 $r_0 = b$ and $V(r) = 0$ so $\theta = 2 \cos^{-1}(\frac{b}{b_{max}})$. b is chosen by $b = b_{max} \sqrt{\gamma}$ where γ is a computer generated random number.

Notice that the hard sphere model has simplified the equation for the scattering angle to an analytically integrable function with a well-behaved solution [9]. This simple computation for the scattering angle significantly decreases the computation time in the Monte Carlo and is a good basis for computational testing and debugging. However, these assumptions also decrease the viability of this model as an accurate representation of the actual molecular collision process.

III.3.2 Lennard-Jones Potential

The Lennard-Jones potential is used to account for Van der Waals potential between particles. The Lennard-Jones potential is commonly used to accurately incorporate an attractive potential term:

$$V_{LJ}(r) = 4\epsilon \left[\left(\frac{\sigma_{LJ}}{r} \right)^{12} - \left(\frac{\sigma_{LJ}}{r} \right)^6 \right] \quad (3)$$

where ϵ is the depth of the attractive potential well and σ is the equilibrium distance at which the potential is zero [9]. Experimental values for ϵ and σ are used. No such experimental values exist for silicon or silane, so values can be conjectured from known values of similar size gases such as argon. The values for σ_{LJ} and ϵ in this simulation are $\sigma_{LJ} = 5.203 * 10^{-10}$ and $\epsilon = 0.04713 \text{ eV } K^{-1}$ [10].

Incorporating the Lennard-Jones potential, the equation for the scattering angle becomes

$$\theta = b \int_{r_0}^{b_{max}} \frac{dr}{r^2 \left[1 - \frac{4\epsilon \left[\left(\frac{\sigma_{LJ}}{r} \right)^{12} - \left(\frac{\sigma_{LJ}}{r} \right)^6 \right]}{E_{COM}} - \left(\frac{b}{r} \right)^2 \right]^{\frac{1}{2}}} \quad (4)$$

This equation is not analytically integrable. The parameters of this equation are $r_0, b_{max}, \sigma_{LJ}$, and ϵ and the independent variables are $E = E_{COM}$ and b .

In order to calculate θ for a Lennard-Jones potential, equation 4 is integrated numerically in Mathematica for values of E in the relevant energy range $0.065 \text{ eV} < E < 0.305 \text{ eV}$ and for values of b between 0 and b_{max} . Polynomial solutions are interpolated for θ vs. b for the range of energies at intervals of 0.02 eV, graphed in Figure 6. The coefficients for these solutions are stored as a look-up table in the program and then referenced to obtain a value for θ from E and b .

Although the energy range $E < 0.065$ is still viable under the parameters of this simulation, at lower energy molecular orbital effects are more prominent and a fit solution is not accurate [10]. In this range a random scattering angle is chosen.

III.4 Variable Soft Sphere Model

The variable soft sphere (VSS) model for particle collisions is widely used to give more accurate results for collision algorithms than the hard sphere model would [4]. This model is a simple modification of the hard sphere model that introduces a parameter α to systematically decrease the scattering angles and effectively "slow down" the thermalization rate of gases modeled with a hard sphere potential. The scattering angle for a variable soft sphere is [4]

$$\theta = 2 \cos^{-1} \left(\left(\frac{b}{b_{max}} \right)^{1/\alpha} \right) \quad (5)$$

IV Results and Discussion

IV.1 χ^2 Comparison of Models

The hard sphere model and the Lennard-Jones model differ in their determination of the scattering angle θ . In the hard sphere model, large scattering angles are more frequent than in the Lennard-Jones model. As in equation 2, a lower scattering angle corresponds to smaller energy transfer, and therefore more collisions are required for thermalization. As a result, simulations with the Lennard-Jones potential take much longer to thermalize and have a different initial energy-dependent thermalization rate than simulations with the hard sphere model as can be seen in Figures 7 and 8.

One goal of this project is to describe this difference in thermalization behavior using a single parameter. To describe how thermalized the test particle gas is after a certain number of collisions the χ^2 value is taken between the velocity distribution of the test gas and the velocity distribution of the background gas, the Maxwell Boltzmann distribution.

$$\chi^2 = \sum_{i=1}^n \frac{(O_i - V_i)^2}{V_i} \quad (6)$$

where O_i is the frequency of the velocity range i for the test gas, V_i is the frequency of that velocity for the MB distribution, and n is the number of data points, or velocity bins in the velocity histogram.

The result of this calculation plotted as a function of the number of collisions N is a decaying exponential function described by $\exp[-\eta(E_0)N]$ where $\eta(E_0)$ is a function of the initial input energy of the test particle.

$\eta(E_0)$ is found to be a linear function of E_0 , so it can be written $\eta(E_0) = \beta E_0$. β is the slope of the fit line of initial input energy vs. thermalization rate, and is the final parameter used to characterize thermalization for different scattering models.

In order to determine if the VSS model is an appropriate computationally inexpensive alternative to the LJ potential, the thermalization rates are compared for varying values of the parameter α in the VSS scattering angle. As α increases, it is expected that the thermalization parameter β will decrease.

IV.2 Results

The χ^2 curves are plotted for the hard sphere and Lennard-Jones models with input initial energies of 0.5eV, 0.75eV, 1.0eV, 1.5eV, and 2eV with a background distribution at 300K and pressure of 10mTorr. The simulations are run for 100000 test particles. The test gas with a hard sphere potential thermalizes after about 12 collisions and the test gas with the LJ potential thermalizes after about 120 collisions. The value of β for the hard sphere is 3.24. The value of β for the LJ potential is 0.23.

Values for β using the VSS potential are found for $\alpha = 1.0, 1.25, 1.5, 1.75, 2.0, 2.5, 3.0, 3.2, 3.5,$ and 4.0 and shown in Figure 9. Note that the value for β_{VSS} at $\alpha = 1.0$ is β_{HS} . For $\alpha < 3$ the results are as expected, where β decreases for increasing α . However, for $\alpha > 3.0$ β asymptotically approaches 1.75.

This result indicates that there is apparently no value for α for the variable soft sphere model that gives the same value for β as the Lennard-Jones potential. The Lennard-Jones potential is thus always a softer potential with a long-term thermalization characteristic.

V Future Work

V.1 Direct Simulation Monte Carlo

The implementation of a Direct Simulation Monte Carlo (DSMC) program is one future goal of this project. In the current test particle Monte Carlo test particles do not interact with each other. A DSMC allows all particles to interact, resulting in a more robust simulation.

The DSMC method divides the represented space into discrete cells. Each molecule is then associated with one of the cells. The program iterates through each cell, chooses a certain number of collision pairs, performs the collision algorithm on these pairs, and updates the velocity of each particle. Then the program increments the position of every particle on the cell based on its velocity vector over a given, predetermined time step. It is possible for a particle to move into another cell after this step. [4] This technique is very computationally expensive, and its implementation is the motivation for finding a method of easily calculating the scattering angle [2].

V.2 Including Chemical Reactions

A more sophisticated version of this program incorporates boundaries for the chamber and initializes test particles by sampling from the MB distribution at 2200K, the temperature of the hot wire. Additionally, each particle has a probability of chemical interaction. If there is no chemical reaction, the test particle collides with the background gas as usual. If there is a chemical interaction, then the particle is removed from the simulation, as the molecular species is transformed. [5][8]. By incorporating chemical reactions, the balance between thermal reactions and chemical reactions can be studied.

V.3 Analysis of Spatial Distribution

The ultimate objective of this program is to determine the flux of various molecular species on the substrate. This is found with the spatial distribution, which can be determined by including an energy-dependent impact parameter into the model and plotting the position histogram for an increasing number of collisions. Analysis of the spatial distribution with the inclusion of chemical reactions and a DSMC method will result in a robust model of film deposition that with control parameters that can be adjusted to maximize deposition rate for high quality silicon films. [3]

VI Conclusion

By determining an appropriate molecular interaction model and implementing a Direct Simulation Monte Carlo method, we can develop a realistic model for molecular flow in hot wire chemical vapor deposition and predict the flux of different molecular species on the substrate. Using such a model to analyze the spatial thermalization distribution will determine how to adjust the parameters in the chamber for a maximum deposition rate of high quality films.

This comparison of thermalization properties of different molecular models indicates that the commonly used variable soft sphere model in gas phase scattering simulations does not exhibit the same thermalization behavior as the Lennard-Jones potential.

However, future work may show that the variable soft sphere potential is a suitable model for determining spatial distribution. It is necessary to include energy dependence in the maximum impact parameter in order to complete this next stage in the development of a viable model for gas phase film deposition.

APPENDIX

Coordinate Transformation

What follows is documentation of the coordinate transformation performed in the collision program. For the following calculations, γ represents a computer generated random number with a seed dependent on time. It is assumed that scattering is isotropic. In spherical coordinates:

$$\theta = \cos^{-1}(2\gamma_1 - 1)$$

$$\phi = 2\pi\gamma_2$$

In order to make the coordinate transformation for calculation of the post-collision velocity in the center of mass frame, the final velocity \mathbf{v} is equal to the components sum in the lab frame and the components sum in the COM frame:

$$\mathbf{v} = v'_x \hat{i}' + v'_y \hat{j}' + v'_z \hat{k}'$$

$$\mathbf{v} = v_x \hat{i} + v_y \hat{j} + v_z \hat{k}$$

The final goal is to obtain \hat{i}' , \hat{j}' , and \hat{k}' in terms of \hat{i} , \hat{j} , and \hat{k} by solving for a_{xx} , a_{xy} , a_{xz} , a_{yx} , a_{yy} , a_{yz} , a_{zx} , a_{zy} , a_{zz} in the following relation:

$$\hat{i}' = a_{xx} \hat{i} + a_{xy} \hat{j} + a_{xz} \hat{k}$$

$$\hat{j}' = a_{yx} \hat{i} + a_{yy} \hat{j} + a_{yz} \hat{k}$$

$$\hat{k}' = a_{zx} \hat{i} + a_{zy} \hat{j} + a_{zz} \hat{k}$$

Given a pre-collision velocity \mathbf{u} , let $\alpha = \frac{u_x}{u}$, $\beta = \frac{u_y}{u}$, and $\gamma = \frac{u_z}{u}$. By forcing $\hat{k}' = \frac{\mathbf{u}}{u}$, gives $a_{zx} = \alpha$, $a_{zy} = \beta$, and $a_{zz} = \gamma$.

Forcing \hat{j}' to be in the yz plane of the lab frame, then $a_{yx} = 0$.

The following relations are true because \hat{i}' , \hat{j}' , and \hat{k}' define an orthonormal basis in the COM frame:

$$\hat{i}' \times \hat{j}' = \hat{k}'$$

$$\hat{i}' \cdot \hat{j}' = 0$$

The result is 5 equations for the remaining unknowns:

$$a_{yy}^2 + a_{yz}^2 = 1 \quad (7)$$

$$a_{xy}a_{yy} + a_{xz}a_{yz} = 0 \quad (8)$$

$$a_{xy}a_{yz} - a_{xz}a_{yy} = a_{zx} \quad (9)$$

$$-a_{xx}a_{yz} = a_{zy} \quad (10)$$

$$a_{xx}a_{yy} = a_{zz} \quad (11)$$

With the final result:

$$\begin{aligned} a_{xx} &= -\sqrt{\beta^2 + \gamma^2} & a_{yx} &= 0 \\ a_{xy} &= -\frac{\alpha\beta}{\sqrt{\beta^2 + \gamma^2}} & a_{yy} &= \frac{\gamma}{\sqrt{\beta^2 + \gamma^2}} \\ a_{xz} &= -\frac{\alpha\gamma}{\sqrt{\beta^2 + \gamma^2}} & a_{yz} &= -\frac{\beta}{\sqrt{\beta^2 + \gamma^2}} \end{aligned}$$

After this transformation is performed, the scattering angle θ and consequent final energy of the test particle T_1 are calculated as in equations (1) and (2).

REFERENCES

1. Branz, H.W., C.W. Teplin, M.J. Romero, I.T. Martin, Q. Wang, K. Alberi, D.L. Young, P. Stradins. *Thin Solid Films*. **519**, 4545-4550 (2011).
2. Prasanth, P.S. and Kakkassery, J.K., *J. Indian Inst. Sci.* **86**, 169-192 (2006).
3. Molenbroek, E.C. and Mahan, A.H. *J. Appl. Phys.* **82**, 1909-1917 (1997).
4. Bird, G.A. *Molecular gas dynamics and the direct simulation of gas flows*. (Clarendon Press, Oxford, 1994).
5. Zheng, W. and Gallagher, A. *Thin Solid Films*. **516**, 929-939 (2008).
6. IUPAC. *Compendium of Chemical Terminology*, 2nd ed. (the "Gold Book"). Compiled by A. D. McNaught and A. Wilkinson. Blackwell Scientific Publications, Oxford (1997).
7. Goodwin, D.G. *Mat. Res. Soc. Symp. Proc.* **557**, 79-84 (1999).
8. Marion, J.B. and Thornton, S.T. *Classical Dynamics of Particles and Systems*. (Brooks Cole, 2003), pp. 291-310.
9. Myers, A.M. *Characterization of the growth flux during the deposition of hydrogenated amorphous silicon by DC magnetron reactive sputtering*. (University of Illinois at Chicago Circle, Chicago, IL, 1984).
10. Hirschfelder, J.O. *Molecular theory of gases and liquids*. (Wiley, New York, NY, 1954).

Figure Captions

Figure 1. A diagram of hot wire chemical vapor deposition. Silane gas is pumped in and reacts off a tantalium or tungsten wire. The opposite plate is often just the chamber wall.

Figure 2. A flowchart of the Test Particle Monte Carlo simulation program. The program is written in C++.

Figure 3. A flowchart of the direct sampling process in the test particle Monte Carlo program to determine the energy of the collision partner of a test particle, chosen from the background gas thermalized at the Maxwell-Boltzmann distribution. The test velocity is a random number between 0 and 5 times the average velocity, or the maximum of the curve (v_{mean})

Figure 4. Demonstrates the direct sampling process from a Maxwell-Boltzmann velocity distribution function at the temperature of the background gas. The x-axis is velocity in m/s and the y-axis is a probability. In this diagram, the velocity distribution is normalized to 1, but in the simulation the range is 1 to 5 times the mean velocity. If point A were chosen in the algorithm for choosing a background particle, it would be rejected and the algorithm would repeat. If point B were chosen, the x-value corresponding to a velocity would be taken as the velocity of the background particle.

Figure 5. Diagram of particle interactions with some non-zero radially-dependent potential. b is the impact parameter. In the simulation, m_1 is the mass of silicon and m_2 is the mass of silane.

Figure 6. This graph is of the fit functions b^2 vs. $1 - \cos(\theta)$ for energy between .065eV and .305eV at intervals of .02eV. $1 - \cos(\theta)$ is on the y-axis and b^2 is on the x-axis. Since the final scattering angle is a function of both the impact parameter and energy, plots are made for several energy values. The plots that appear with higher values on the graph correspond to a lower energy. The interpolated polynomials that describe these graphs are used in the final simulation to determine the scattering angle with a Lennard-Jones potential.

Figure 7. Thermalization evolution of test particles with the Hard Sphere potential. Plotted against the Maxwell-Boltzmann distribution depicted in blue, which corresponds to the velocity distribution of the background gas.

Figure 8. Thermalization evolution of test particles with the Lennard-Jones potential. The top graph approximates a delta function at the initial energy of the test particles, 1eV. Plotted against the Maxwell-Boltzmann distribution depicted in blue, which corresponds to the velocity distribution of the background gas.

Figure 9. Thermalization characterization values β for the variable soft sphere potential plotted against the scattering parameter α from the Variable Soft Sphere potential.

Figures

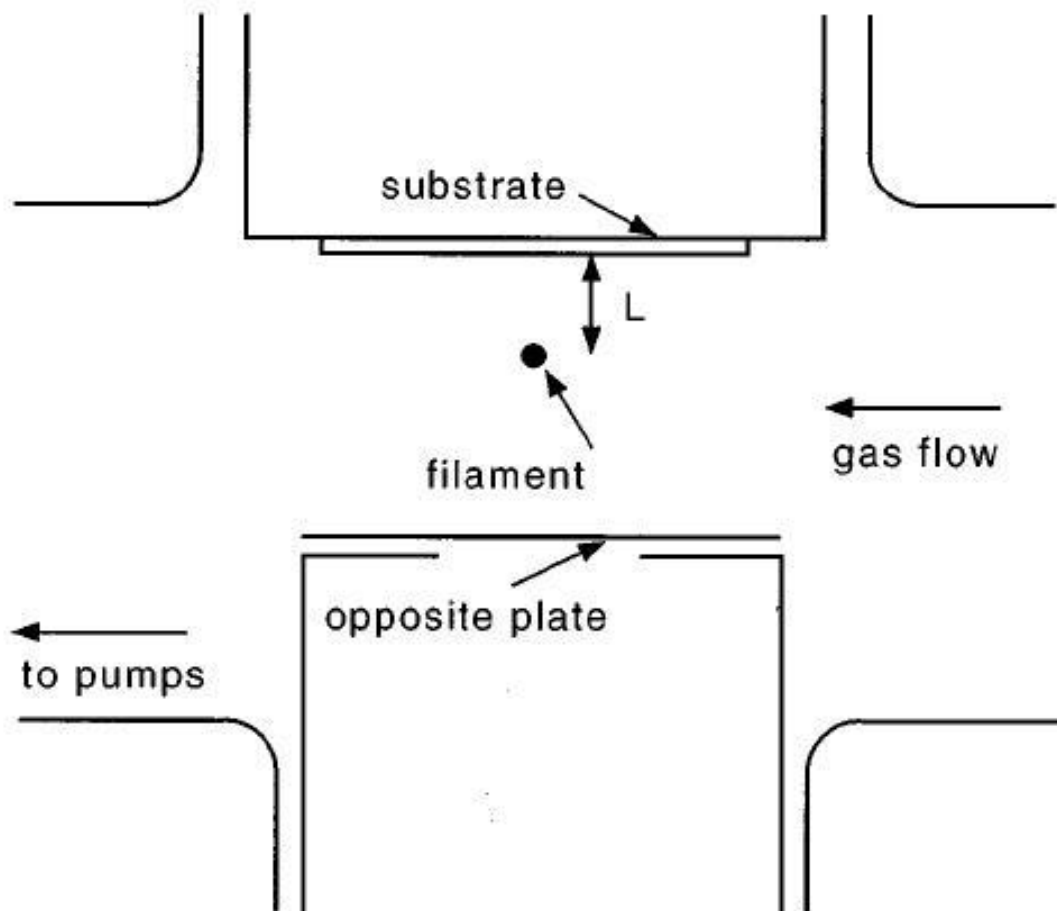


Figure 1

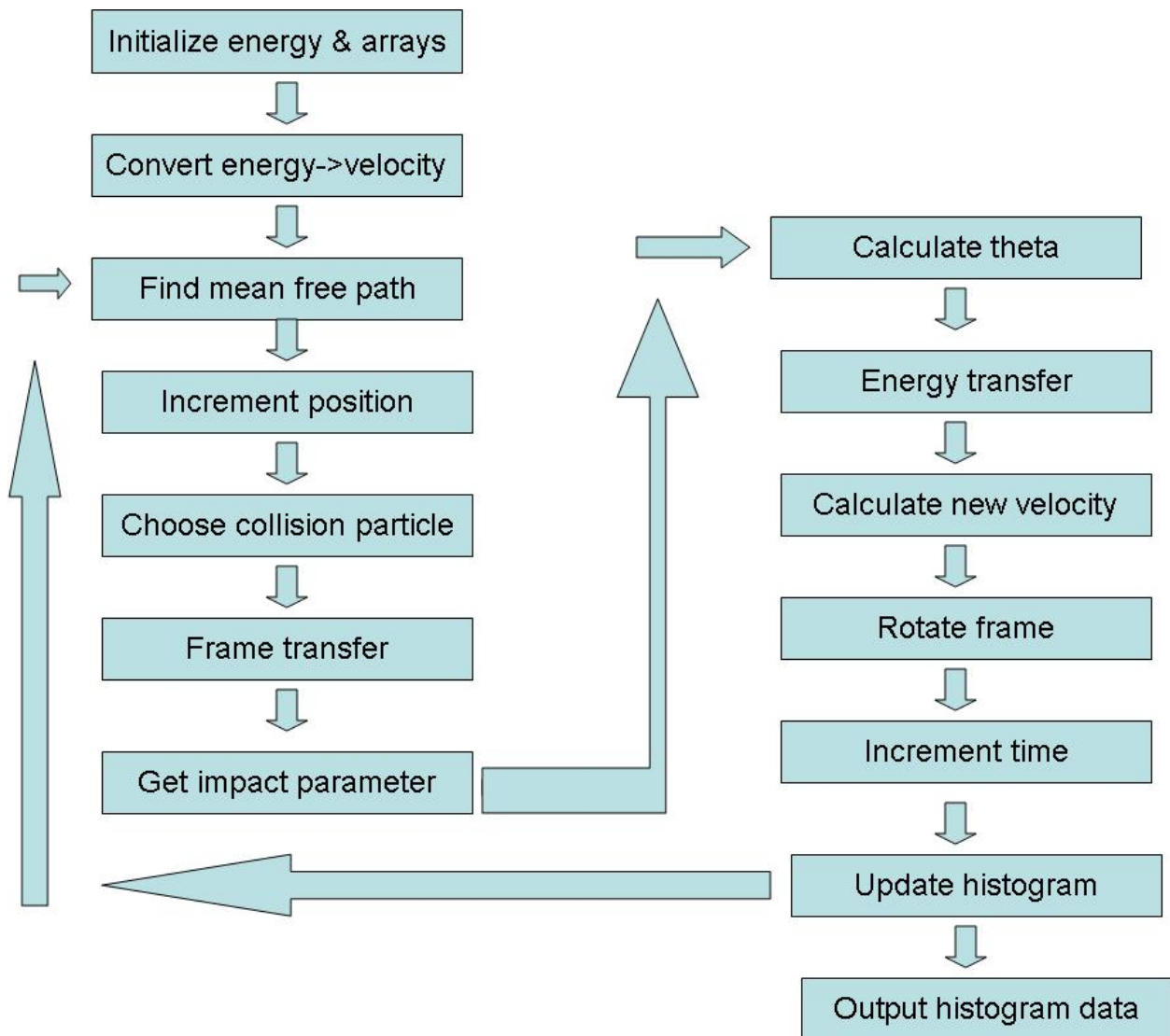


Figure 2

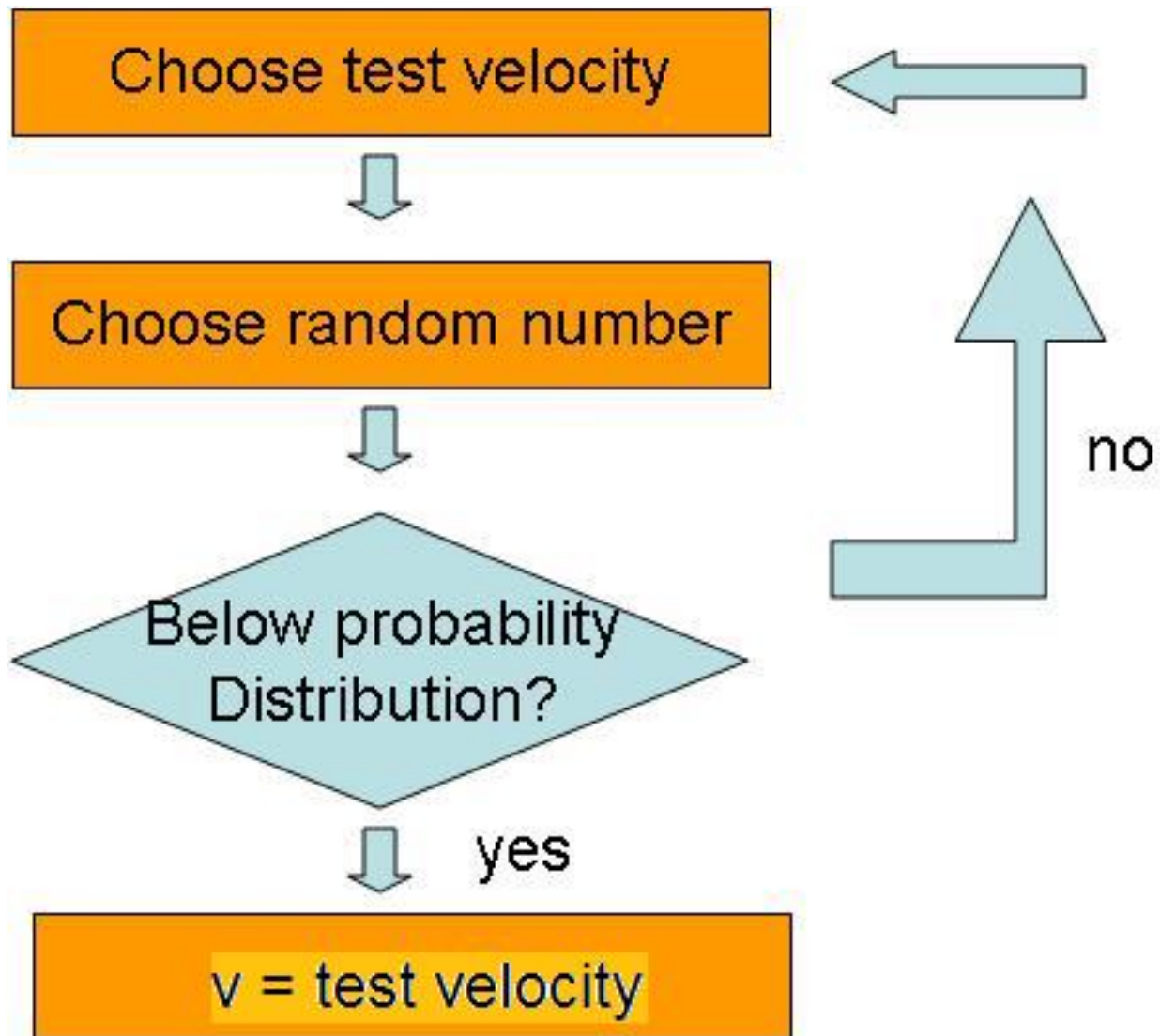


Figure 3

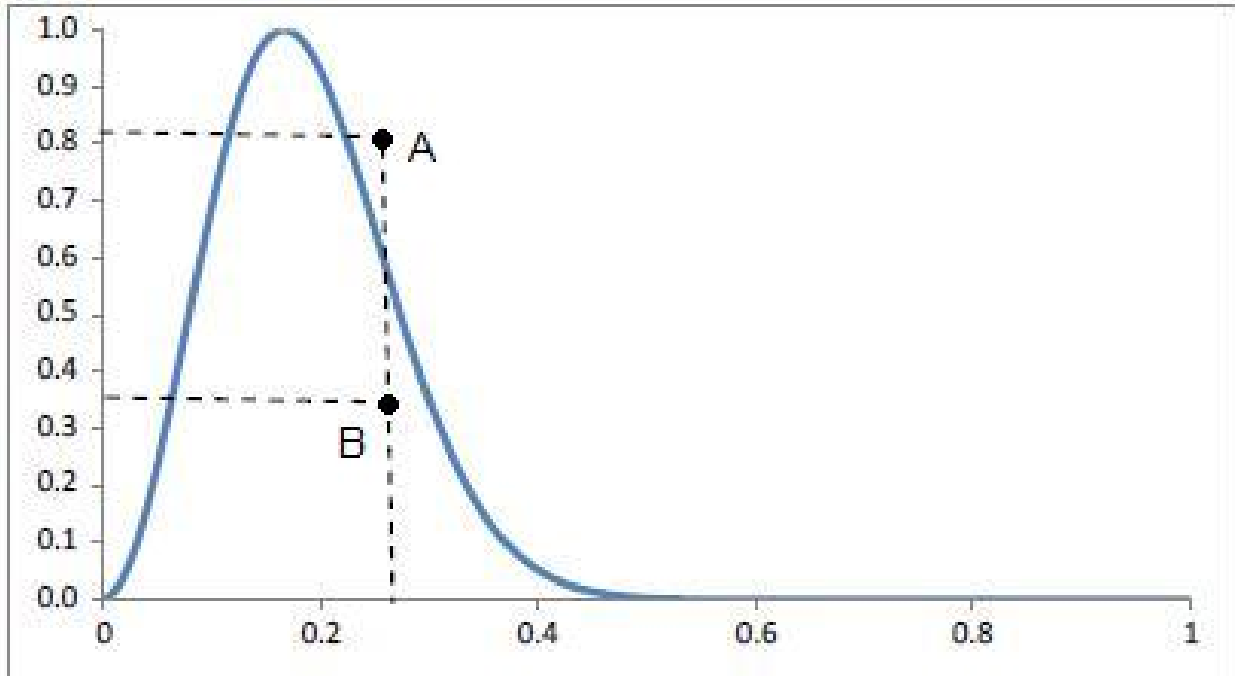


Figure 4

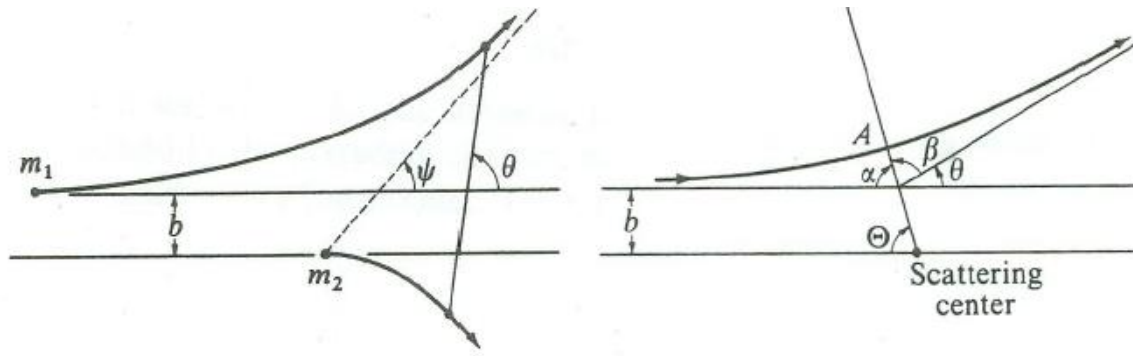


Figure 5

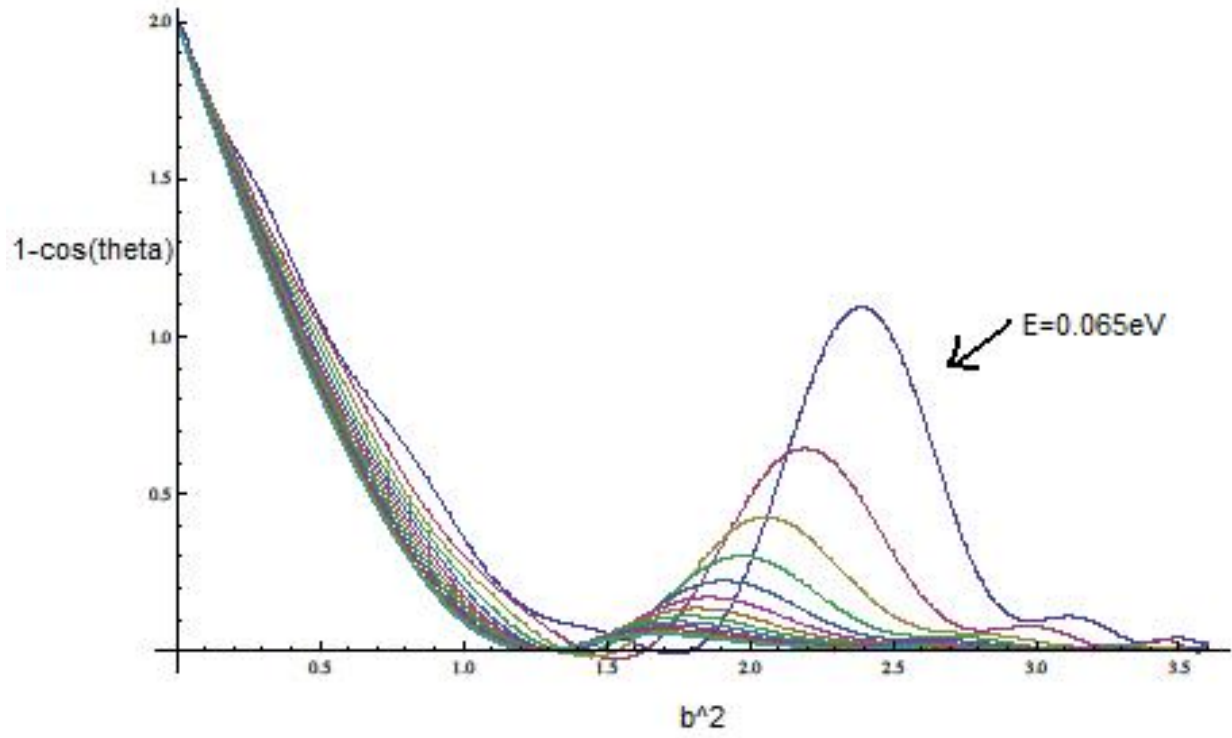


Figure 6

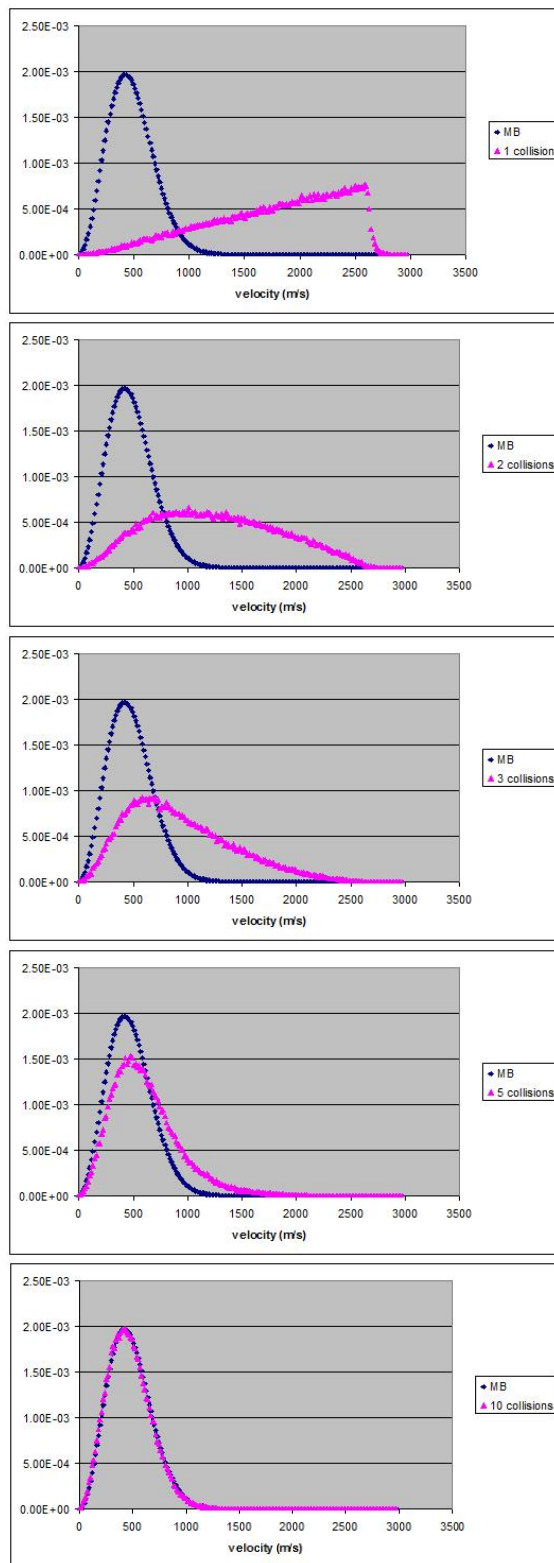


Figure 7

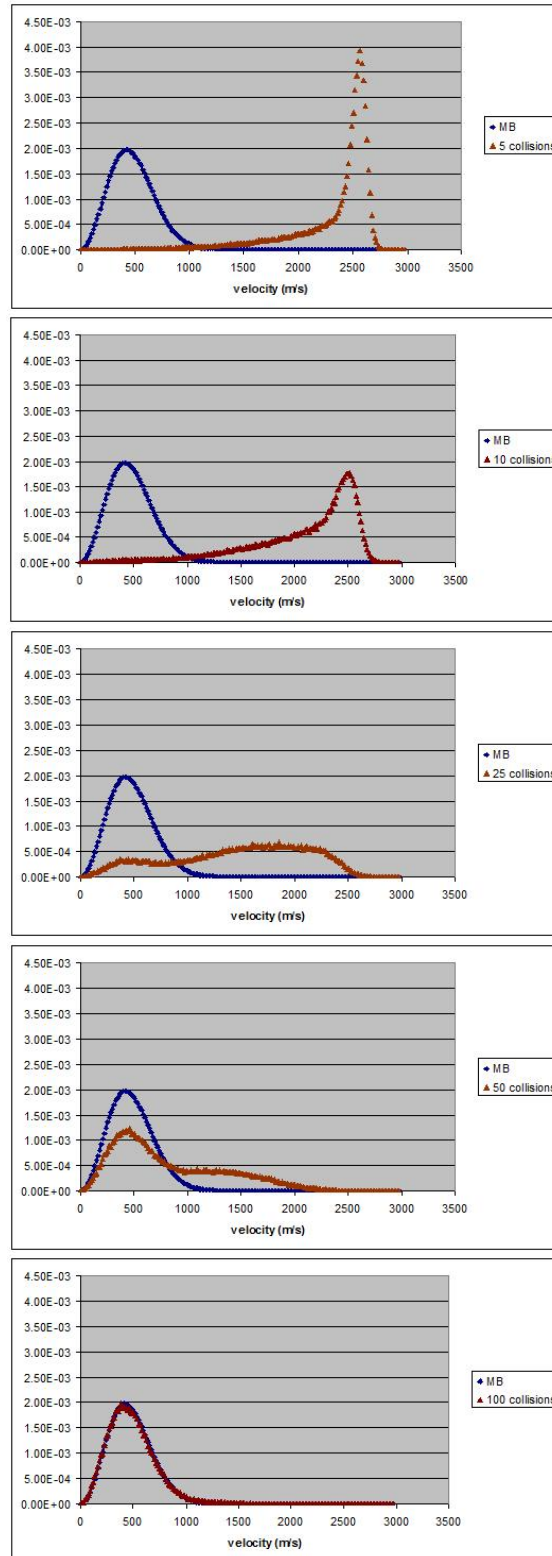


Figure 8

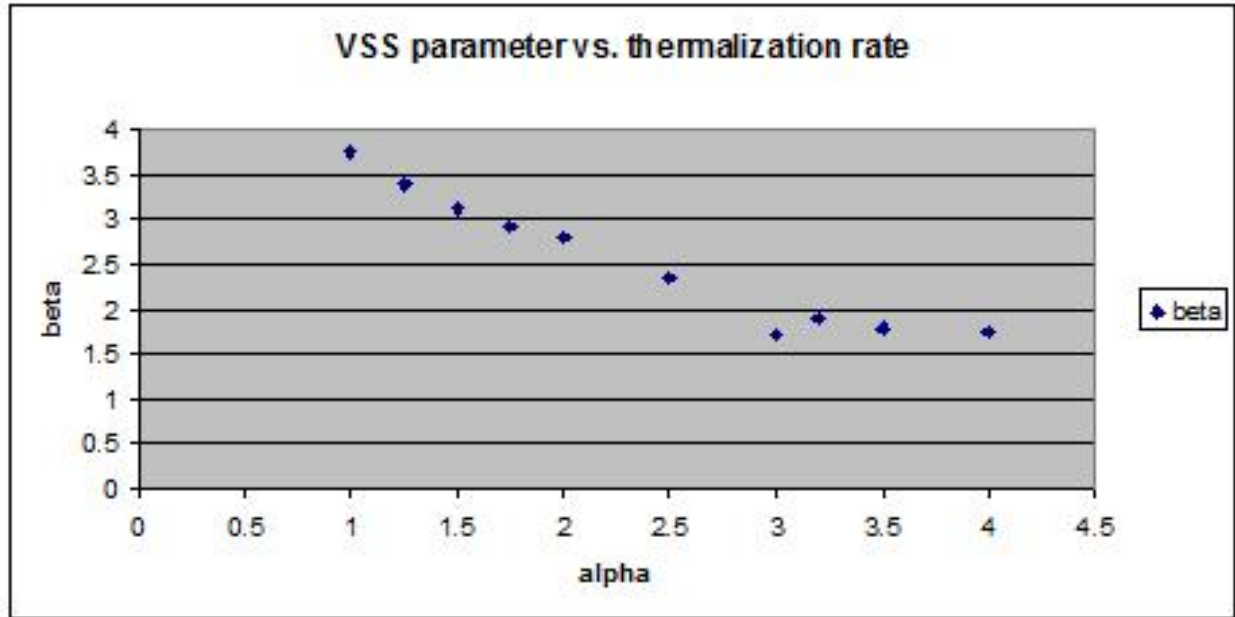


Figure 9